Sensitivity Analysis of Transmissibility Functions for Structural Damage Detection

Dapeng Zhu, Xiaohua Yi, Yang Wang *
School of Civil and Environmental Eng., Georgia Inst. of Technology, Atlanta, GA 30332, USA

ABSTRACT

In order to assess structural safety conditions, many vibration-based damage detection methods have been developed in recent years. Among these methods, transmissibility function analysis can utilize output data only, and proves to be effective in damage detection. However, previous research mostly focused on experimental validation of using transmissibility function for damage detection. Very few studies are devoted to analytically investigating its performance for damage detection. In this paper, a spring-mass-damper model with multiple degrees-of-freedom is formulated for further analytical studies on the damage sensitivity of transmissibility functions. The sensitivity of transmissibility function against structural mass and stiffness change is analytically derived and validated by numerical examples.

Keywords: Transmissibility function analysis, structural damage detection, spring-mass-damper model

1. INTRODUCTION

Large-scale civil structures, such as bridges, dams, and high-rise buildings, may be subjected to severe natural disasters or harsh operational environment. Structural condition may deteriorate significantly over the life cycle. Taking bridges as an example, an ASSHTO [1] report mentioned that "while 50 years ago the nation faced a historic period of bridge construction, today it faces a historic period of bridge repair and reconstruction." According to the ASCE 2009 report on America's infrastructure [2], more than one fourth of the bridges in the United States are categorized as structurally deficient or functionally obsolete. It was estimated that a $17 billion annual investment is needed to substantially improve the bridge conditions, yet currently, only $10.5 billion is spent annually on the construction and maintenance of bridges. In order to efficiently utilize available resources and prioritize retrofit tasks, there is a pressing demand for reliable techniques that are capable of diagnosing structural conditions.

In recent years, various damage detection algorithms have been developed for identifying the existence of damage in structures [3]. Among these methods, transmissibility function analysis attracted considerable interest due to its effectiveness in damage identification and requirement for output data only. A number of researchers investigated the application of transmissibility function analysis. For example, Zhang *et al.* used translational and curvature transmissibility functions to locate damage on a composite beam [4]. The effects of operational and environmental variability on the transmissibility function analysis were analyzed by Kess and Adams [5]. Their work suggested that the damage detection accuracy based on transmissibility function could be improved by identifying specific frequency ranges that are more sensitive to damage and immune to sources of uncertainties. Devriendt and Guillaume [6] concluded that arbitrary forces could be used to perform the transmissibility-function-based operational modal analysis, as long as the structure is persistently excited in the frequency range of interest. Zhu *et al.* [7] successfully employed transmissibility function analysis to detect damage on a laboratory frame using data collected by mobile sensing nodes. Nevertheless, little research has been devoted to exploring the nature of transmissibility functions for damage detection in an analytical manner. For example, Johnson and Adams explored the explicit formulation of transmissibility functions using a three degrees-of-freedom (DOFs) system [8]. However, analytical formulation of transmissibility functions for structures with an arbitrary large number of DOFs has not been reported.

This study investigates the analytical formulation for the damage sensitivity of transmissibility functions based on a general multi-DOF spring-mass-damper system. For the multi-DOF system, the transmissibility functions are expressed in recursive form using symbolic inversion of tri-diagonal matrices. Section 2 of this paper presents an analytical

* yang.wang@ce.gatech.edu; phone 1 404 894-1851; fax 1 404 894-2278; http://www.ce.gatech.edu/~ywang

derivation for the damage sensitivity of transmissibility functions, which illustrates the potential of using change in transmissibility functions to identify and locate damage. Two types of damage scenarios are studied. The first scenario considers mass change, and the second scenario considers stiffness loss. Section 3 presents the numerical simulation results that validate the conclusion from the derivation. A five-story shear-building model is built in ANSYS, which is equivalent to a 5-DOF spring-mass-damper system. The two types of damage scenarios discussed in Section 2 are studied in the simulation. Section 4 summarizes this paper and discusses future research work.

2. TRANSMISSIBILITY FUNCTION ANALYSIS FOR A MULTI-DOF SPRING-MASS-DAMPER SYSTEM

In this section, the transmissibility function for a multi-DOF spring-mass-damper system is first analytically derived. The sensitivity of the transfer function for two damage scenarios is then studied. The first damage scenario considers mass change, and the second damage scenario considers stiffness loss.

2.1 Transmissibility function for a multi-DOF spring-mass-damper system

For a multi-DOF spring-mass-damper system (Figure 1), the equations of motion can be formulated as:

$$\mathbf{M}\ddot{\mathbf{x}}(t) + \mathbf{C}\dot{\mathbf{x}}(t) + \mathbf{K}\mathbf{x}(t) = \mathbf{f}(t) \tag{1}$$

where $\mathbf{x}(t)$, $\dot{\mathbf{x}}(t)$ and $\ddot{\mathbf{x}}(t)$ denote the displacement, velocity and acceleration vectors of the system, respectively. $\mathbf{f}(t)$ denotes the external excitation; **M**, **C,** and **K** are the mass, damping and stiffness matrices, respectively, which can be expressed as the follows:

$$\mathbf{M} = \mathrm{Diag}\{m_1, m_2, \cdots, m_N\} \tag{2}$$

$$\mathbf{K} = \begin{bmatrix} k_1 + k_2 & -k_2 & 0 & 0 & \cdots & 0 \\ & k_2 + k_3 & -k_3 & 0 & \cdots & 0 \\ & & \ddots & \ddots & \ddots & \vdots \\ & & & k_{N-2} + k_{N-1} & -k_{N-1} & 0 \\ & \text{Sym.} & & & k_{N-1} + k_N & -k_N \\ & & & & & k_N + k_{N+1} \end{bmatrix} \tag{3}$$

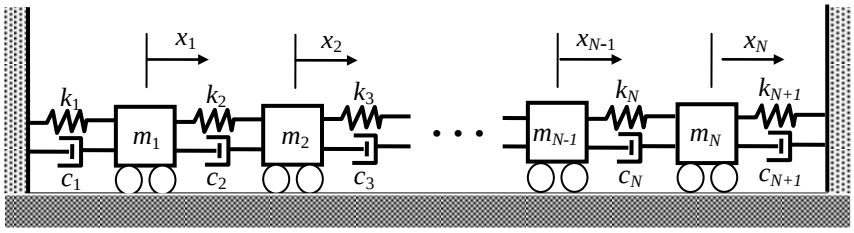

Figure 1. A multi-DOF spring-mass-damper system

$$\mathbf{C} = \begin{bmatrix} c_1 + c_2 & -c_2 & 0 & 0 & \cdots & 0 \\ & c_2 + c_3 & -c_3 & 0 & \cdots & 0 \\ & & \ddots & \ddots & \ddots & \vdots \\ & & & c_{N-2} + c_{N-1} & -c_{N-1} & 0 \\ & \text{Sym.} & & & c_{N-1} + c_N & -c_N \\ & & & & & c_N + c_{N+1} \end{bmatrix} \tag{4}$$

Here "Diag" denotes a diagonal matrix, and "Sym." denotes the symmetric part of a matrix.

Applying the Laplace transform (assuming zero initial condition), the time-domain formulation can be converted to:

$$\mathbf{X}(s) = \mathbf{H}(s)\mathbf{F}(s) \tag{5}$$

where $\mathbf{H}(s)$ is known as the transfer function matrix and s is the complex variable.

The acceleration vector in the complex domain can be expressed as:

$$\mathbf{A}(s) = s^2\mathbf{H}(s)\mathbf{F}(s) \tag{6}$$

The transmissibility function $T_{ij}(s)$ between the output i and reference-output j is defined as the ratio of two acceleration responses $A_i(s)$ and $A_j(s)$. Let $\mathbf{h}(s)$ denote one row of $\mathbf{H}(s)$, then

$$T_{ij}(s) = \frac{A_i(s)}{A_j(s)} = \frac{s^2\mathbf{h}_i(s)\mathbf{F}(s)}{s^2\mathbf{h}_j(s)\mathbf{F}(s)} = \frac{\mathbf{h}_i(s)\mathbf{F}(s)}{\mathbf{h}_j(s)\mathbf{F}(s)} \tag{7}$$

If only one external excitation $f_k(t)$ is applied to the k-th DOF of the structure, Equation (7) can be further simplified since the external excitation is canceled out:

$$T_{ij}(s) = \frac{H_{ik}(s)}{H_{jk}(s)} \tag{8}$$

Thus, the transmissibility function $T_{ij}(s)$ is determined by two entries in the transfer matrix, $H_{ik}(s)$ and $H_{jk}(s)$. It is known that the transfer matrix $\mathbf{H}(s)$ is equal to the inverse of matrix $\mathbf{B}(s)$, where

$$\begin{aligned} \mathbf{B}(s) &= s^2\mathbf{M} + s\mathbf{C} + \mathbf{K} \\ &= \begin{bmatrix} m_1 s^2 + (c_1 + c_2)s + k_1 + k_2 & -c_2 s - k_2 & 0 & \cdots & 0 \\ & m_2 s^2 + (c_2 + c_3)s + k_2 + k_3 & -c_3 s - k_3 & \cdots & 0 \\ & & \ddots & \ddots & \vdots \\ & \text{Sym.} & & \ddots & -c_N s - k_N \\ & & & & m_N s^2 + (c_N + c_{N+1})s + k_N + k_{N+1} \end{bmatrix} \end{aligned} \tag{9}$$

Note that matrix $\mathbf{B}$ is a symmetric tridiagonal matrix.

According to [9], the entries of $\mathbf{H}(s)$ can be expressed in a recursive form:

$$H_{ij} = \begin{cases} U_i \cdots U_{j-1} H_{jj} & i < j \\ H_{ji} & i > j \\ [B_{ii} - X_i - Y_i]^{-1} & i = j \end{cases} \tag{10}$$

where the intermediate variables are computed as:

$$U_i = -[B_{ii} - Y_i]^{-1} B_{i(i+1)} \qquad (i = 1, \cdots, N-1)$$
$$Y_i = \begin{cases} 0 & (i = 1) \\ B_{i(i-1)}^2 \, [B_{(i-1)(i-1)} - Y_{i-1}]^{-1} & (i = 2, \cdots, N) \end{cases} \tag{11}$$
$$X_i = \begin{cases} 0 & (i = N) \\ B_{i(i+1)}^2 \, [B_{(i+1)(i+1)} - X_{i+1}]^{-1} & (i = 1, \cdots, N-1) \end{cases}$$

From Equation (11), the recursive relationship between U_i and $U_{i\text{-}1}$ can be derived as:

$$U_i = \frac{-B_{i(i+1)}}{B_{ii} + B_{i(i-1)} U_{i-1}} \qquad (i = 2, ..., N\text{-}1) \tag{12}$$

Consider a special case in which acceleration measurements are taken at two neighboring DOFs at a time, following the sequence 1 and 2, 2 and 3, …, (*N*-1) and *N*. For each measurement at two neighboring DOFs, an external excitation is applied at the latter DOF in the pair. For example, the measurement is taken at DOFs 2 and 3, when the excitation is applied at DOF-3. In this case, according to Equations (8) and (10), the transmissibility functions between each two neighboring DOFs can be expressed as:

$$T_{i(i+1)} = \frac{H_{i(i+1)}}{H_{(i+1)(i+1)}} = \frac{U_i H_{(i+1)(i+1)}}{H_{(i+1)(i+1)}} = U_i, \quad i = 1, 2, \cdots, N-1 \tag{13}$$

From Equation (11), when *s* is large enough, U_1 can be simplified as

$$U_1 = \frac{-B_{12}}{B_{11}} = -\frac{-c_2 s - k_2}{m_1 s^2 + (c_1 + c_2) s + k_1 + k_2} \approx \frac{c_2}{m_1 s} \tag{14}$$

Substituting Equation (14) into Equation (12), when *s* is large enough, U_2 can be simplified as

$$U_2 = \frac{-B_{23}}{B_{22} + B_{12} U_1} \approx -\frac{-c_3 s - k_3}{m_2 s^2 + (c_2 + c_3) s + k_2 + k_3 + (-c_2 s - k_2) \dfrac{c_2}{m_1 s}} \approx \frac{c_3}{m_2 s} \tag{15}$$

Similarly, when *s* is large enough, such that

$$\left| m_i s^2 \right| >> \left| (c_i + c_{i+1}) s \right| \text{ and } \left| c_i s \right| >> k_i \qquad \text{for } \forall i \tag{16}$$

the denominator and the numerator of U_i are dominated by the term with the highest power of *s*, and U_i can be approximately expressed as

$$U_i \approx \frac{c_{i+1}}{m_i s} \tag{17}$$

The difference between the transmissibility functions of the undamaged structure and the damaged structure, ε_i, is used for damage detection.

$$\varepsilon_i = T_{i(i+1)}^D - T_{i(i+1)} = U_i^D - U_i \tag{18}$$

where the superscript "^{D}" refers to the damaged structure.

A damage indicator can be defined as the sum of the absolute value of ε_i in certain frequency range of ω:

$$DI_i = \sum_k \left| \varepsilon_i (s_k) \right| \tag{19}$$

where $s_k = \mathrm{j}\omega_k$ and j is the imaginary unit.

2.2 Damage scenario I – mass change

In damage scenario I, suppose that damage occurs at DOF n, with the mass m_n changed to m_n^D. In experimental studies, a mass change, which affects structural dynamics properties, is often used to represent a reversible damage. According to Equation (9), only entry B_{nn} in **B** matrix will change due to the damage, and all other entries remain the same. Let B_{nn}^D denote the corresponding entry in **B** matrix with the changed mass. From Equation (12), it is concluded that after the damage, U_i will remain the same for $i < n$, and will change to U_i^D for $i \geq n$.

The difference in transmissibility functions, ε_i, can be categorized into three cases by different measurement locations (Figure 2), and simplified when s is large enough (i.e. when the inequalities in Equation (16) holds).

Case I (a) $i < n$

As shown in Figure 2(a), the measurement is taken at two neighboring DOFs i and i+1, while the external excitation is applied at DOF i+1, with $i < n$. As previously described, U_i will remain unchanged after damage, for $i < n$. From Equation (18), the transmissibility function difference ε_i is equal to zero in this case, which means the mass change at DOF n does not cause change in transmissibility function T_{ij} ($i < n$).

Case I (b) $i = n$

As shown in Figure 2(b), the measurement is taken at two neighboring DOFs n and n+1, while the external excitation is applied at DOF n+1. As previously described, when $i = n$, B_{nn} is the only term in Equation (12) that changes due to the damage, and $U_{n\text{-}1}$ will remain unchanged after damage. Substituting Equation (12) into Equation (18), the transmissibility function difference $\varepsilon_i = \varepsilon_n$ can be derived as:

$$\begin{aligned} \varepsilon_n = U_n^D - U_n &= \frac{-B_{n(n+1)}}{B_{nn}^D + B_{n(n-1)}U_{n-1}} - \frac{-B_{n(n+1)}}{B_{nn} + B_{n(n-1)}U_{n-1}} \\ &= \frac{B_{n(n+1)}\left(B_{nn}^D - B_{nn}\right)}{\left(B_{nn}^D + B_{n(n-1)}U_{n-1}\right)\left(B_{nn} + B_{n(n-1)}U_{n-1}\right)} \end{aligned} \tag{20}$$

Substituting Equation (14) into the above, when s is large enough, ε_n can be simplified as:

$$\varepsilon_n \approx \frac{-c_{n+1}\left(m_n^D - m_n\right)}{m_n^D m_n s} \tag{21}$$

This means the mass change at DOF n causes change in transmissibility function $T_{n(n+1)}$.

Case I (c) $i > n$

As shown in Figure 2(c), the measurement is taken at two neighboring DOFs i and i+1, while the external excitation is

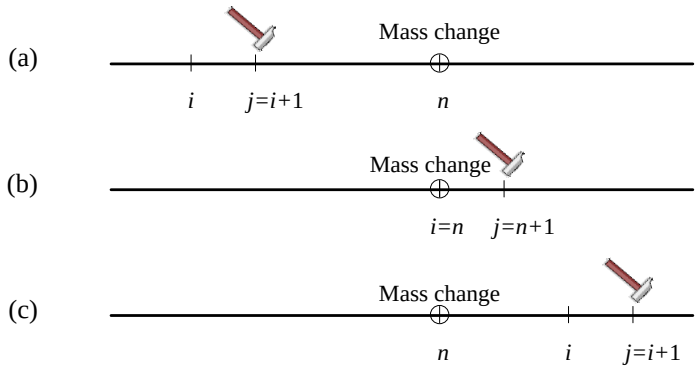

Figure 2. Mass change at DOF n, while measurements are taken at DOFs i and i+1.The external excitation is applied at DOF i+1: (a) $i < n$; (b) $i = n$; (c) $i > n$

applied at DOF i+1 ($i > n$). As previously described, when $i > n$, the B_{**} terms in Equation (12) remain unchanged due to damage, and only the U_{i-1} term changes. Substituting Equation (12) into Equation (18), the transmissibility function difference ε_i can be derived as:

$$\begin{aligned}\varepsilon_i &= U_i^D - U_i = \frac{-B_{i(i+1)}}{B_{ii} + B_{i(i-1)}U_{i-1}^D} - \frac{-B_{i(i+1)}}{B_{ii} + B_{i(i-1)}U_{i-1}} \\ &= \frac{B_{i(i+1)}B_{i(i-1)}\varepsilon_{i-1}}{\left(B_{ii} + B_{i(i-1)}U_{i-1}^D\right)\left(B_{ii} + B_{i(i-1)}U_{i-1}\right)}\end{aligned} \tag{22}$$

Substituting Equation (14) into the above, when s is large enough, ε_i can be simplified as:

$$\varepsilon_i \approx \frac{c_i c_{i+1}}{m_i^2 s^2}\varepsilon_{i-1} \tag{23}$$

This means that when the measurement locations move further away from the mass change, the transmissibility function difference caused by damage reduces at the rate of s^{-2} after every pair of measurement locations.

In summary, when $i < n$, the transmissibility functions are not affected by the damage and the difference ε_i remains zero; when $i = n$, for large s, the transmissibility function difference ε_n approximately has the order of s^{-1}; when $i > n$, for large s, ε_i decreases at the rate of s^{-2} as DOF i increases. Therefore, we can conclude that in higher frequency range (note that $s = j\omega$), the transmissibility function difference at the damage location, ε_n, should be approximately the largest. All other transmissibility function differences, $\varepsilon_i (i \neq n)$, should be relatively small. As a result, the damage indicator, DI_i, as defined in Equation (19), should be approximately the largest when $i = n$, i.e. when the excitation and measurement are next to the damage (Figure 2(b)).

2.3 Damage scenario II – stiffness loss

In damage scenario II, suppose that damage occurs between DOFs n-1 and n, as the stiffness reduction from k_n to k_n^D. According to Equation (9), only entries $B_{(n-1)(n-1)}$, $B_{(n-1)n}$, $B_{n(n-1)}$ and B_{nn} in **B** matrix will change due to the damage, and

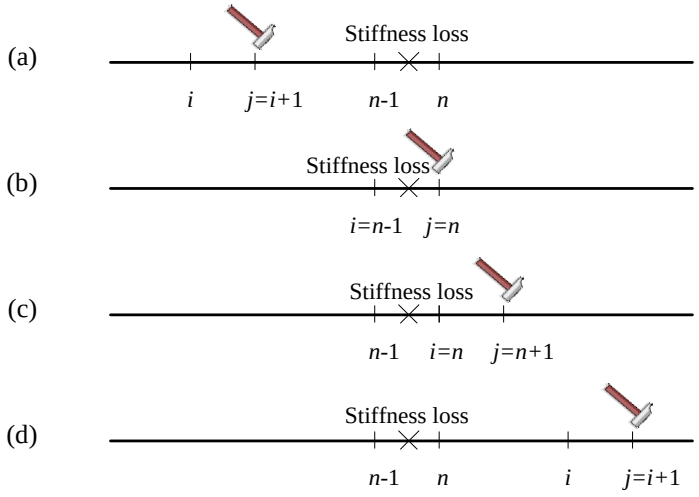

Figure 3. Stiffness loss between DOFs n-1 and n, while measurements are taken at DOFs i and i+1. An external excitation is applied at DOF i+1: (a) $i < n$-1; (b) $i = n$-1; (c) $i = n$; (d) $i > n$

all other entries remain the same. Let $B^D_{(n-1)(n-1)}$, $B^D_{(n-1)n}$, $B^D_{n(n-1)}$ and B^D_{nn} denote the corresponding entries in **B** matrix with stiffness loss. Again from Equation (12), it is concluded that after the damage, U_i will remain the same for $i<n$-1, and will change to U_i^D for $i \geq n$-1.

The difference in transmissibility functions, ε_i, can be categorized into four cases by different measurement locations (Figure 3), and simplified when s is large enough (i.e. when the inequalities in Equation (16) holds).

Case II (a) $i < n$-1

As shown in Figure 3(a), the measurement is taken at two neighboring DOFs i and i+1, while the external excitation is applied at DOF i+1, with $i < n$-1. As previously described, U_i will remain unchanged after damage, for $i < n$-1. From Equation (18), the transmissibility function difference ε_i is equal to zero in this case, which means the damage does not cause change in transmissibility function T_{ij} ($i < n$-1).

Case II (b) $i = n$-1

As shown in Figure 3(b), the measurement is taken at two neighboring DOFs n-1 and n, while the external excitation is applied at DOF n. As previously described, when $i = n$-1, $B_{(n-1)(n-1)}$ and $B_{(n-1)n}$ are the only terms in Equation (12) that change due to the damage, and U_{n-2} will remain unchanged after damage. Substituting Equation (12) into Equation (18), the transmissibility function difference $\varepsilon_i = \varepsilon_{n-1}$ can be derived as:

$$\begin{aligned}\varepsilon_{n-1} &= U^D_{n-1} - U_{n-1} = \frac{-B^D_{(n-1)n}}{B^D_{(n-1)(n-1)} + B_{(n-1)(n-2)}U_{n-2}} - \frac{-B_{(n-1)n}}{B_{(n-1)(n-1)} + B_{(n-1)(n-2)}U_{n-2}} \\ &= \frac{B_{(n-1)n}B^D_{(n-1)(n-1)} - B^D_{(n-1)n}B_{(n-1)(n-1)} + \left(B_{(n-1)n} - B^D_{(n-1)n}\right)B_{(n-1)(n-2)}U_{n-2}}{\left(B^D_{(n-1)(n-1)} + B_{(n-1)(n-2)}U_{n-2}\right)\left(B_{(n-1)(n-1)} + B_{(n-1)(n-2)}U_{n-2}\right)}\end{aligned} \tag{24}$$

Substituting Equation (14) into the above, when s is large enough, ε_{n-1} can be simplified as:

$$\varepsilon_{n-1} \approx \frac{(k^D_n - k_n)}{m_{n-1}s^2} \tag{25}$$

This means the transmissibility function difference caused by damage has the order of s^{-2} in this case.

Case II (c) $i = n$

As shown in Figure 3(c), the measurement is taken at two neighboring DOFs n and n+1, while the external excitation is applied at DOF n+1. As previously described, when $i = n$, B_{nn}, $B_{n(n-1)}$ and U_{n-1} are the terms in Equation (12) that change due to the damage. Substituting Equation (12) into Equation (18), the transmissibility function difference $\varepsilon_i = \varepsilon_n$ can be derived as:

$$\begin{aligned}\varepsilon_n &= U^D_n - U_n = \frac{-B_{n(n+1)}}{B^D_{nn} + B^D_{n(n-1)}U^D_{n-1}} - \frac{-B_{n(n+1)}}{B_{nn} + B_{n(n-1)}U_{n-1}} \\ &= \frac{B_{n(n+1)}\left(B^D_{nn} - B_{nn} + B^D_{n(n-1)}U^D_{n-1} - B_{n(n-1)}U_{n-1}\right)}{\left(B^D_{nn} + B^D_{n(n-1)}U^D_{n-1}\right)\left(B_{nn} + B_{n(n-1)}U_{n-1}\right)}\end{aligned} \tag{26}$$

Substituting Equation (14) into the above, when s is large enough, ε_n can be simplified as:

$$\varepsilon_n \approx \frac{-c_{n+1}\left(k^D_n - k_n\right)}{m^2_n s^3} \tag{27}$$

This means the transmissibility function difference caused by damage has the order of s^{-3} in this case.

Case II (d) $i > n$

As shown in Figure 3(d), the measurement is taken at two neighboring DOFs i and i+1, while the external excitation is applied at DOF i+1 ($i > n$). As previously described, when $i > n$, the B_{**} terms in Equation (12) remain unchanged due to damage, and only the U_{i-1} term changes. Substituting Equation (12) into Equation (18), the transmissibility function difference ε_i can be derived as:

$$\begin{aligned}\varepsilon_i &= U_i^D - U_i = \frac{-B_{i(i+1)}}{B_{ii} + B_{i(i-1)}U_{i-1}^D} - \frac{-B_{i(i+1)}}{B_{ii} + B_{i(i-1)}U_{i-1}} \\ &= \frac{B_{i(i+1)}B_{i(i-1)}\varepsilon_{i-1}}{\left(B_{ii} + B_{i(i-1)}U_{i-1}^D\right)\left(B_{ii} + B_{i(i-1)}U_{i-1}\right)}\end{aligned} \tag{28}$$

Substituting Equation (14) into the above, when s is large enough, ε_i can be simplified as:

$$\varepsilon_i \approx \frac{c_i c_{i+1}}{m_i^2 s^2}\varepsilon_{i-1} \tag{29}$$

Similar as Case I(c), this means that when the measurement locations move further away from the damage, the transmissibility function difference caused by damage reduces at the rate of s^{-2} after every pair of measurement locations.

In summary, when $i < n$-1, the transmissibility functions are not affected by the damage and the difference ε_i remains zero; when $i = n$-1, for large s, the transmissibility function difference ε_{n-1} approximately has the order of s^{-2}; when $i = n$, for large s, the transmissibility function difference ε_n approximately has the order of s^{-3}; when $i > n$, for large s, the transmissibility function difference ε_i decreases at the rate of s^{-2} as i increases. Therefore, we can conclude that in higher frequency range, the transmissibility function difference ε_{n-1} at the damage location should be approximately the largest and ε_n the second largest. All other transmissibility function differences, $\varepsilon_i (i \neq n, n-1)$, should be relatively small. As a result, the damage indicator, DI_i, as defined in Equation (19), should be approximately the largest when $i = n$-1, i.e. when the measurement locations are at two sides of the stiffness loss(Figure 3(b)).

3. NUMERICAL SIMULATION

To validate the analytical studies in Section 2, a five-story shear-building model is built in ANSYS for simulating a 5-DOF spring-mass-damper system. The two types of damage scenarios discussed in Section 2 are studied. The first damage scenario considers an additional mass fixed at the second floor, and the second damage scenario considers 20% stiffness loss introduced to the elements of one column between the 2nd and 3rd floors.

3.1 Finite element model

Figure 4 shows the five-story shear-building model in ANSYS. Simulating a laboratory structure, the columns are steel and the floors are aluminum. The dimension of each floor is identical: 12 in. long, 12 in. wide and 0.5 in. thick. The two columns have the same rectangular section (6 in. × 0.008 in.). The total height of the building is 60 in., with 12 in. per story. Each floor is connected with the columns through rigid constraints. Fixed boundary conditions are adopted at the bases of the two columns. The material properties of the floors and columns are listed in Table 1. This five-story building model is equivalent to a 5 DOF spring-mass-damper system, because the floor stiffness is much larger than the stiffness of the columns. Modal superposition algorithm is used for dynamics simulation, and 4% modal damping is assigned

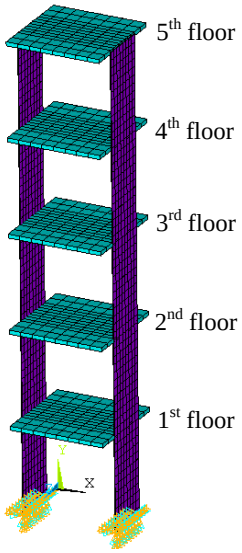

Figure 4. A five-story shear-building model in ANSYS for simulating a 5-DOF spring-mass-damper system.

for each mode. The first five natural frequencies of the shear building are 2.98, 8.78, 14.09, 18.43, and 21.31 Hz.

To follow the measurement scheme described in Section 2, assume two accelerometers are used for measuring horizontal floor vibration every time. Acceleration measurements are taken for floor pairs 1-2, 2-3, 3-4, and 4-5 in sequence. For each measurement, an ideal impact excitation is applied at the higher floor. For example, the measurement is taken at the 2nd and 3rd floors, when the excitation is applied at the 3rd floor. The sampling rate is set to 1,000 Hz, and each measurement duration is set to 10 seconds.

Table 1. Material properties of the five-story shear-building model

Material properties	*Floor*	*Column*
Young's modulus (ksi)	10,000 (aluminum)	29,000 (steel)
Poisson's ratio	0.3	0.3
Density (lb/in^3)	0.098	0.285

Figure 5 plots the acceleration data at the 2nd and 3rd floors when the ideal impact is applied at the 3rd floor of the undamaged structure. Figure 6 shows the magnitude of the two frequency spectra, i.e. the fast Fourier transform (FFT)

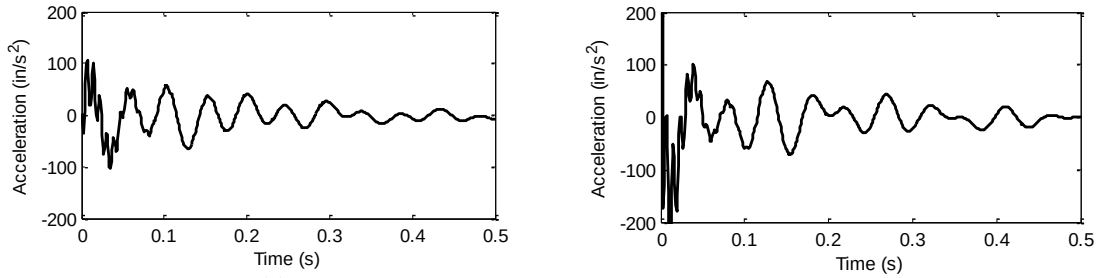

Figure 5. Example acceleration time histories when the hammer impact is applied at the 3rd floor: (a) acceleration at the 2nd floor; (b) acceleration at the 3rd floor.

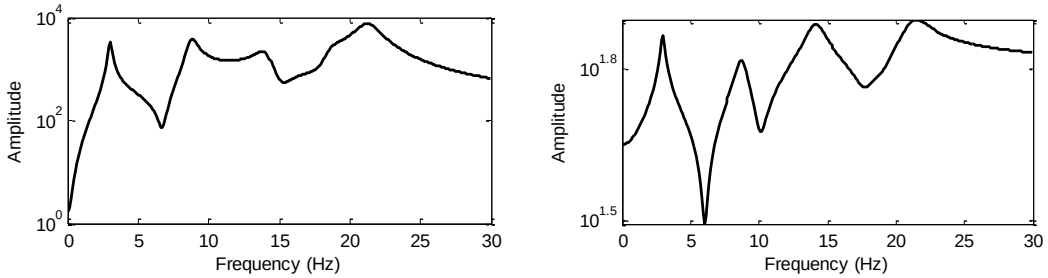

Figure 6. Example acceleration spectra when the hammer impact is applied at the 3rd floor: (a) acceleration spectra at the 2nd floor; (b) acceleration spectra at the 3rd floor.

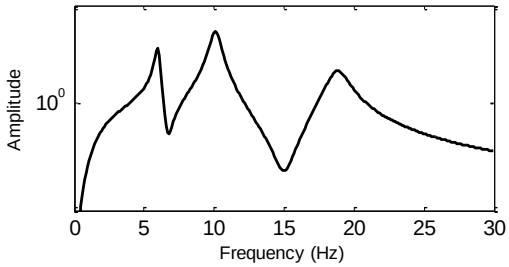

Figure 7. Transmissibility function T_{23} calculated using the example acceleration data.

results of the acceleration time history. According to the definition (Equation (7)), transmissibility function T_{23} is calculated as the ratio between the two frequency spectra, as shown in Figure 7.

3.2 Damage scenario I – additional mass

In damage scenario I, a mass block of 1 lb is attached on the 2nd floor (Figure 8). In contrast, the weight of the each floor is about 7 lbs. With the mass block attached, acceleration records are sequentially obtained at floor pairs 1-2, 2-3, and so on. Same as the measurement scheme for the undamaged structure, for each floor pair, an ideal impact is applied at the higher floor in the pair.

After obtaining all the acceleration records, the transmissibility functions T_{12}, T_{23}, T_{34}, and T_{45} for both the undamaged and damaged structures are calculated. Figure 9 presents the magnitude of the transmissibility functions of both the undamaged and damaged structures. It is shown that $|T_{12}|$ and $|T_{12}^{D}|$ are almost the same at any frequency range. At higher frequency range, e.g. 25~30Hz, $|T_{23}|$ and $|T_{23}^{D}|$ have the largest difference. This agrees with the conclusion from the analytical formulation in Section 2.2.

The damage indicators are calculated based on the transmissibility function difference in frequency range 25~500Hz (Equation (19)), and shown in Figure 10. The largest damage indicator is $DI_{2\text{-}3}$, and the other damage indicators are much smaller, which again agrees with conclusion made in section 2.2, i.e. the largest damage indicator occurs next to the damage location.

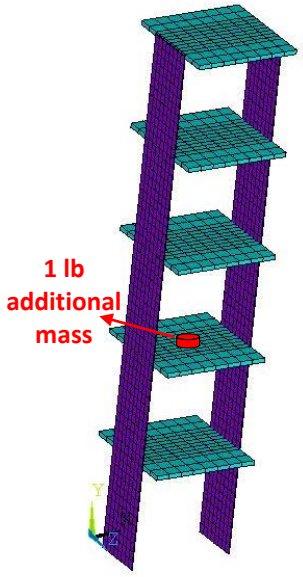

Figure 8. Damage scenario I – A 1lb additional mass is attached on the 2nd floor.

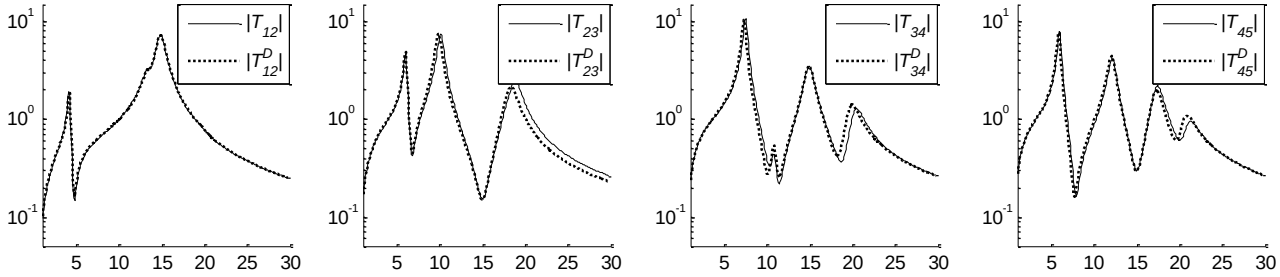

Figure 9. Comparison of transmissibility functions between undamaged and damaged (scenario I) structures

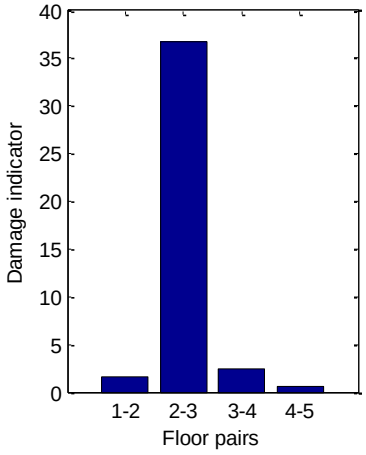

Figure 10. Damage scenario I - the damage indicators at four measurement floor pairs

3.3 Damage scenario II – stiffness loss

In damage scenario II, a 20% stiffness loss is introduced to the elements of one column between the 2nd and 3rd floors (Figure 11). After the stiffness loss, acceleration records are sequentially obtained at floor pairs 1-2, 2-3, and so on. Same as the measurement scheme for the undamaged structure, for each floor pair, an ideal impact is applied at the higher floor in the pair.

After obtaining all the acceleration records, the transmissibility functions T_{12}, T_{23}, T_{34}, and T_{45} for both the undamaged and damaged structures are calculated. Figure 12 presents the magnitude of the transmissibility functions of both the undamaged and damaged structures. It is shown that $|T_{12}|$ and $|T_{12}^{D}|$ are almost the same at any frequency range. At higher frequency range, e.g. 25~30Hz, $|T_{23}|$ and $|T_{23}^{D}|$ have the largest difference. This also agrees with the conclusion from the analytical formulation in Section 2.3.

The damage indicators are also calculated based on the transmissibility function difference in frequency range 25~500Hz (Equation (19)), and shown in Figure 13. The largest damage indicator is $DI_{2\text{-}3}$, the second largest is $DI_{3\text{-}4}$, and all other damage indicators are much smaller, which again agrees with the conclusion made in section 2.3, i.e. the largest damage indicator occurs near the damage location.

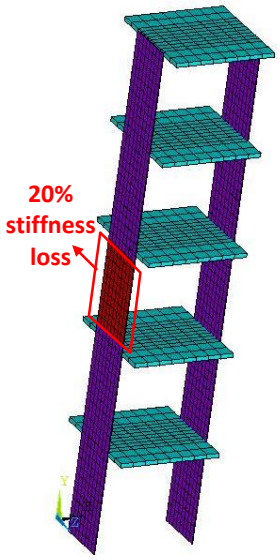

Figure 11. Damage scenario II – 20% stiffness loss is introduced to the elements of one column between 2nd and 3rd floors.

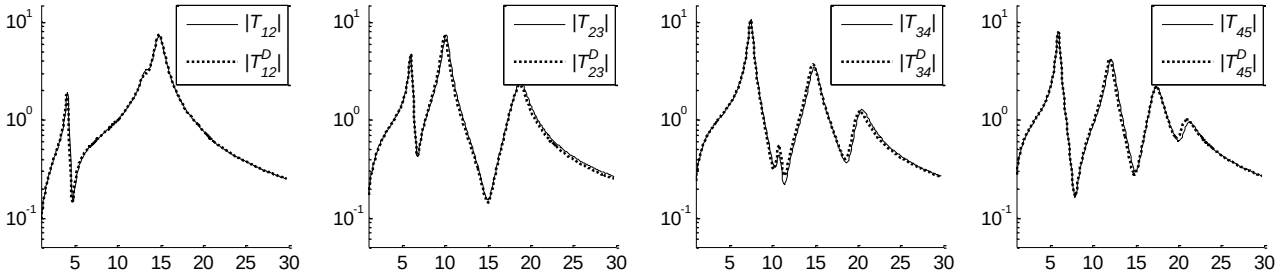

Figure 12. Comparison of transmissibility functions between undamaged and damaged (scenario II) structures

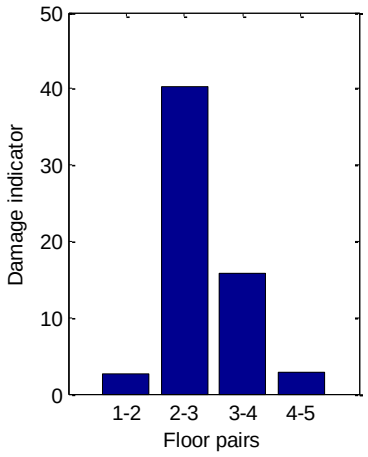

Figure 13. Damage scenario II - the damage indicators at four measurement floor pairs

4. SUMMARY AND DISCUSSION

Using a multi-DOF spring-mass-damper system, this study investigates the analytical derivation for structural damage detection using changes in transmissibility function. Two damage scenarios are considered. The first damage scenario considers mass change, and the second damage scenario considers stiffness loss. Analytical derivations show that the difference in transmissibility functions between undamaged and damaged structures is sensitive to both damage scenarios and can be used for damage identification and localization. With the proposed measurement and excitation scheme, the largest damage indicator should approximately occur near the damage location. To validate the analytical derivations, numerical simulation is conducted, where a five-story shear-building model is built in ANSYS for simulating a 5-DOF spring-mass-damper system. For both damage scenarios, transmissibility function analysis is applied, and damage identification results agree with the conclusion from the analytical study.

Future research can be focused on the experimental validation for this analytical study. Another interesting topic is to identify multiple damage occurrences in a multi-DOF spring-mass-damper system using transmissibility functions. Besides, more complex structural models, e.g. trusses or frames, need to be investigated for analytically studying the damage sensitivity of the transmissibility functions.

ACKNOWLEDGEMENT

This research is partially sponsored by the National Science Foundation, under grant number CMMI-0928095 (Program Manager: Dr. Shih-Chi Liu). The authors gratefully acknowledge the support.

REFERENCES

[1] AASHTO, *Bridging the Gap*. American Association of State Highway & Transportation Officials, Washington D.C. (2008).

[2] ASCE, *Report Card for America's Infrastructure*, American Society of Civil Engineers, Reston, VA (2009).

[3] Doebling, S.W., Farrar, C.R., Prime, M.B. and Shevitz, D.W., *Damage Identification and Health Monitoring of Structural and Mechanical Systems from Changes in their Vibration Characteristics: a Literature Review*. Report No. LA-13070-MS, Los Alamos National Laboratory, Los Alamos, NM (1996).

[4] Zhang, H., Schulz, M.J., Ferguson, F. and Pai, P.F., "Structural health monitoring using transmittance functions," *Mech. Syst. Signal Pr.* , 13(5), 765-787 (1999).

[5] Kess, H.R. and Adams, D.E., "Investigation of operational and environmental variability effects on damage detection algorithms in a woven composite plate," *Mech. Syst. Signal Pr.*, 21(6), 2394-2405 (2007).

[6] Devriendt, C. and Guillaume, P., "Identification of modal parameters from transmissibility measurements," *J. Sound Vib.*, 314(1-2), 343-356 (2008).

[7] Zhu, D., Yi, X., Wang, Y., Lee, K.-M. and Guo, J., "A mobile sensing system for structural health monitoring: design and validation," *Smart Mater. Struct.*, 19(5), 055011 (2010).

[8] Johnson, T.J. and Adams, D.E., "Transmissibility as a differential indicator of structural damage," *J. Vib. Acoust.*, 124(4), 634-641 (2002).

[9] Godfrin, E.M., "A method to compute the inverse of an N-block tridiagonal quasi-Hermitian matrix " *J. Phys.: Condens. Matter*, 3(40), 7843-7848 (1991).